Optical constants and thickness determination of very thin amorphous semiconductor films

I. Chambouleyron[a*], S. D. Ventura[b], E. G. Birgin[c] and J. M. Martínez[b]

[a] *Institute of Physics 'Gleb Wataghin', State University of*

Campinas–UNICAMP,

P.O.Box 6165, 13083-870 Campinas, SP, Brazil

[b] *Institute of Mathematics and Computer Science,*

State University of Campinas – UNICAMP,

P.O.Box 6065, 13083-970 Campinas, SP, Brazil

[c] *Dept. Computer Science, IME – University of São Paulo – USP,*

Rua do Matão 1010, 05508-900 São Paulo, SP, Brazil

(April 13, 2006)

Typeset using REVTEX

Optical constants and thickness determination of very thin amorphous semiconductor films

I. Chambouleyron*, S. D. Ventura, E. G. Birgin and J. M. Martínez

Abstract

This contribution addresses the relevant question of retrieving, from transmittance data, the optical constants and thickness of very thin semiconductor and dielectric films. The retrieval process looks for a thickness that, subject to the physical input of the problem, minimizes the difference between the measured and the theoretical spectra. This is a highly underdetermined problem but, the use of approximate – though simple – functional dependences of the index of refraction and of the absorption coefficient on photon energy, used as an a priori information, allows surmounting the ill-posedness of the problem. The method is illustrated with the analysis of transmittance data of very thin amorphous silicon films. The method allows retrieving physically meaningful solutions for films as thin as 300Å. The estimated parameters agree well with known data or with optical parameters measured by independent methods. The limitations of the adopted model and the shortcomings of the optimization algorithm are presented and discussed.

* Corresponding author; e-mail ivanch@ifi.unicamp.br

A. Introduction

Today, advanced electronic and optical devices are manufactured involving the deposition of single or multilayered structures of materials, including all kind of semiconductors, dielectrics, nitrides, oxides, and other alloys. Frequently, the thickness of these mostly amorphous or polycrystalline thin layers is just a few tens of nanometers. The optical properties of very thin films are different from those of the corresponding bulk material, the difference stemming either from materials' inhomogeneities or, as the thickness of the films decreases, from the increasing influence of surface and interface defective layers. As the true optical properties of the deposited films may influence the overall device performance, the need appears to develop fast and accurate characterization methods to extract the optical constants and the thickness of such very thin coatings. Measurements of the complex amplitudes of the light transmitted and reflected at normal or oblique incidence at the film and substrate sides, or different combinations of them, enable the explicit evaluation of the thickness and the optical constants in a broad spectral range. At normal incidence, the planes of equal phase are parallel to those of equal amplitude for isotropic absorbing films. The formulation of the problem becomes more involved at non-normal incidence. Normal reflectance is not easily available in standard equipments. This is not the case of normal transmittance, which provides quick, accurate and non-destructive information on material's properties in a spectral range going from complete opacity to transparency – an interesting photon energy range for many applications.

The retrieval of the optical properties and thickness of a thin film from transmittance data is a reverse optical engineering problem in the sense that the response of the system is known but the parameters producing this response must be estimated [1]. This is a highly underdetermined ill-posed problem, the solution not being unique. As shown in this, and in previous publications [2,3], the ill-posedness can be surmounted by introducing in the

3

problem some prior information on the behavior of the parameters to be estimated. In the present contribution we address and solve the problem of extracting the optical properties and thickness from the transmission spectra of amorphous semiconductor layers as thin as 300 Å. The reliability and limitations of the retrieval process are discussed.

Sometimes, the properties of relatively thick films can be obtained from transmission spectra quite accurately with the so-called envelope methods [4–7]. The main shortcoming of such methods, however, is that they cannot be used in the case of rather thin films, because their transmittance does not display an interference fringe pattern at photon energies corresponding to zero, or almost zero, absorption . In recent publications, we reported two approaches – a pointwise constrained optimization approach [2] and a pointwise unconstrained optimization approach (PUM) [3,8] – that proved to be very useful to circumvent the difficulty of a lacking fringe pattern. Both methods minimize the difference between measured and calculated transmittance introducing, with ad hoc procedures, some prior knowledge of the physically meaningful solution. The optimization algorithms were tested with computer simulated films [3] and with amorphous semiconductor films deposited onto glass substrates [8]. In all cases, the methods proved to be highly reliable for films thickness in excess of ≈ 100 nm.

In this contribution we extend the applicability of the pointwise unconstrained minimization method to the retrieval of the optical constants and the thickness of very thin amorphous semiconductor films, i.e., to film thickness less than 100 nm. We apply a new minimization algorithm to a series of hydrogen-free (a-Si) and hydrogenated amorphous silicon films (a-Si:H) of several thicknesses. The retrieved optical properties agree with published data and/or expected values, the retrieved thicknesses being always close to measured values or to values estimated from deposition rate and deposition time. The method proves its usefulness for film thickness down to 30 nm. The method can be extended without difficulty to other homogeneous films like epitaxial crystalline and organic thin layers.

The paper is organized as follows. Section B introduces the problem and the strategy for the estimation of the optical properties and thickness of very thin amorphous semiconductor

4

films. Section C gives a brief description of the experimental conditions and the main results. Section D contains the discussion of the results considering retrieved optical properties and thickness. The limitations of the approach are also discussed. The conclusions of the work are presented at the end of the paper.

B. The optical model and the retrieval algorithm

The driving idea behind the method allowing the retrieval of the optical constants and the thickness of very thin amorphous semiconductor films is the fact that, for the photon energy range corresponding to transmittance spectra, the absorption coefficient and the index of refraction can be approximated by simple expressions. For example, the absorption edge of amorphous semiconductors and dielectrics films can be broken into two main contributions [10–12]:

$$\alpha = B^2 (h\nu - E_G)^m / h\nu, \ \ \text{for } (h\nu > E_G), \tag{1}$$

with m =2 or 3; and

$$\alpha = A \ exp[(h\nu - E_0)/E_U], \ \ \text{for} \ \ (h\nu < E_0). \tag{2}$$

The quantity α is the absorption coefficient, $h\nu$ denotes photon energy, B is a constant that includes information of the convolution of the valence and conduction band states and on the matrix elements of optical transitions, E_G is the Tauc's optical gap [11], E_U is the characteristic energy of the exponential absorption edge, which depends on the topological disorder of the network [10], and A and E_0 are constants that depend on material composition and deposition method and conditions. At photon energies below the exponential absorption edge a third contribution to α appears, which tends to flattens the absorption curve. This

5

sub-gap absorption originates from transitions between deep localized electron states in the pseudo-gap and extended states in the conduction and in the valence bands. As a consequence, the $log[\alpha(h\nu)]$ versus $h\nu$ plot has an elongated $\int$-like shape, that remembers the integral mathematical symbol [12].

Similarly, within the photon energy range normally given by transmittance measurements, the dependence of the index of refraction on photon energy can be well described using a single-effective-oscillator formulation:

$$n^2 - 1 = E_d E_{osc}/[E_{osc}^2 - (h\nu)^2] \tag{3}$$

where E_{osc} is the single-oscillator energy and E_d is the dispersion energy [13,14]. The expression (3) holds for photon energies well below E_{osc}. At energies approaching E_{osc}, deviations to the simple law (3), originating from the proximity of the main band-to-band transitions, are measured.

Consider now the four-layer situation depicted in Fig. 1: *air (n_0)/film $(\widetilde{n}_f)$/thick transparent substrate (n_S)/air (n_0)*. For simplicity of notation let us call d, n and κ the thickness, the refractive index and the attenuation coefficient of the film, and s the refractive index of the substrate. In this case, the transmittance reduces to [6]:

$$T^{meas}(\lambda) = \text{Measured transmittance} = \frac{Ax}{B - Cx + Dx^2} \tag{4}$$

where:

$$A = 16s(n^2 + \kappa^2) \tag{5}$$

$$B = [(n+1)^2 + \kappa^2][(n+1)(n+s^2) + \kappa^2] \tag{6}$$

$$C = [(n^2 - 1 + \kappa^2)(n^2 - s^2 + \kappa^2) - 2\kappa^2(s^2 + 1)] \, 2\cos\varphi$$

$$-\kappa[2(n^2 - s^2 + \kappa^2) + (s^2 + 1)(n^2 - 1 + \kappa^2)] \, 2\sin\varphi \tag{7}$$

6

$$D = [(n-1)^2 + \kappa^2][(n-1)(n-s^2) + \kappa^2] \tag{8}$$

$$\varphi = 4\pi n d/\lambda, \quad x = exp(-\alpha d), \quad \alpha = 4\pi\kappa/\lambda. \tag{9}$$

The problem of retrieving the extinction coefficient κ, the refractive index n and the thickness d of a thin film from transmittance data is, evidently, highly under-determined. The input of the problem is a set of experimental values $[\lambda_i, T^{meas}(\lambda_i)]$, $\lambda_{\min} \leq \lambda_i \leq \lambda_{i+1} \leq \lambda_{\max}$, for $i = 1, ..., N$. For all wavelengths and a repeating d the following equation must hold:

$$T^{theor}(\lambda) = T^{meas}(\lambda, s(\lambda), d, n(\lambda), k(\lambda)) \tag{10}$$

where T^{theor} is the calculated transmission of the film+substrate structure. This equation has two unknowns, $n(\lambda)$ and $k(\lambda)$, and, in general, its set of solutions (n, k) is a curve in the two-dimensional $[n(\lambda), k(\lambda)]$ space. Consequently, the set of functions (n, k) satisfying $T^{theor} = T^{meas}$ for a given d is infinite. However, as shown in [2], physical constraints (PCs) drastically reduce the range of variability of the unknowns $n(\lambda), k(\lambda)$. For example, in the case of amorphous semiconductors films in the neighborhood of the fundamental edge, typical physical constraints (PC) could be: PC1: $n(\lambda) \geq 1$ and $k(\lambda) \geq 0$ for all $\lambda \in [\lambda_{\min}, \lambda_{\max}]$; PC2: $n(\lambda)$, and $k(\lambda)$ are decreasing functions of (λ); PC3: $n(\lambda)$ is convex; PC4: there exists $\lambda_{\inf l} \in [\lambda_{\min}, \lambda_{\max}]$ such that $k(\lambda)$ is convex if $\lambda \geq \lambda_{\inf l}$ and concave if $\lambda < \lambda_{\inf l}$. These constraints on the unknowns can be eliminated by a suitable change of variables, as shown in detail in [3]. The use of the pointwise unconstrained minimization approach –PUM– needs the calculation of complicate derivatives of functions, which requires the use of automatic differentiation techniques. The present authors used the procedures for automatic differentiation described in [15].

The optimization process looks for a thickness that, subject to the physical input of the problem, minimizes the difference between the measured and the theoretical spectra, i.e.,

7

$$Minimize \sum_{all\ i} [T^{meas}(\lambda_i) - T^{theor}(\lambda_i, s, d, n(\lambda_i), k(\lambda_i))]^2 \qquad (11)$$

The minimization of (11) starts sweeping a thickness range Δd_R divided into thickness steps Δd_s and proceeds decreasing Δd_R and Δd_s until the optimized thickness d_{opt} is found. An example of the process is shown in Fig.2 where $\sum_{all\ i} [T^{meas}(\lambda_i) - T^{theor}(\lambda_i, s, d, n(\lambda_i), k(\lambda_i))]^2$ versus thickness has been plotted for a film with $d = 72$ nm. The left part of Fig. 2 shows the results of a coarse 50 nm step scan. The right part of the figure is an enlargement of the region around the minimum quadratic error found with the coarse step scan, but using a smaller (1 nm) scan step. The absolute minimum corresponds to a thickness of 72 nm, considered the true thickness of the film..

The minimization uses a very simple algorithm introduced recently by Raydan [16], which realizes a very effective idea for potentially large-scale unconstrained minimization. It consists of using only gradient directions with step-lengths that ensure rapid convergence. Let us remember here that the PUM formulation was able to retrieve correctly the thickness, the index of refraction and the absorption coefficient of both computer generated films [3] and hydrogenated amorphous silicon films deposited onto glass [8]. However, it was unable to retrieve physically meaningful solutions from the transmittance of real a-Si:H films of thickness less than 100 nm and of $d < 80$ nm computer generated films. In the present contribution we introduce a new formulation that solves this difficulty and allows retrieving the optical properties and thickness of amorphous semiconductor films having a thickness as small as 30 nm. Needless to say, for such very thin films the properties of surfaces and interfaces influence the overall retrieval, as discussed in the coming sections.

1. Strategy

As the physical thickness of films decreases the information contained in their transmittance decreases. The reason is easy to understand. In the limit of zero thickness (i.e., no film at all) the measured transmittance is just that of the substrate alone. Hence, as this limiting zero thickness is approached, the estimation of film properties becomes more and

more difficult. This situation is typical of the so-called *inverse problems.* In cases where the available information becomes scarce, it is important to add some *a priori* information in the estimation process. Normally, "true" *a priori* information is not available and, therefore, "reasonable" – though not necessarily true – information is incorporated in order to get an estimation. Classical regularization [17] is a typical example of this methodology. In classical regularization, an artificial bound for the solution of an inverse problem is produced, without guaranteeing the correctness of such a bound. In fact, the determination of the correct regularization parameter, which is correlated with the bound, is an involved mathematical and statistical problem. The general practical principle of inverse problems seems to be: if you do not have enough information to determine the solution, adding some "reasonable" – though not necessarily true – information is better than not introducing any information at all. Of course, it is not useful adding "reasonable" information to problems that are sufficiently determined. In the present case, the "reasonable" – though not necessarily true – information is represented by a functional form imposed to the absorption coefficient and to the index of refraction. Probably, real parameters do not follow exactly these functional forms, but the functions are sufficient to eliminate very arbitrary possible solutions.

Our objective is to estimate the optical constants and the thickness of very thin films given a measured spectral transmittance (λ_i, T_i^{meas}), $i = 1, \ldots, N$, with $d < 100$ nm. For such a purpose we adopt a calculation strategy, heretofore called FFM, that was successfully tested with computer generated semiconductor and dielectric films [9].

A model function for the optical constants of these films is such that:

(a) The quantity $1/[n^2(h\nu) - 1]$ is a linear function of $(h\nu)^2$.

(b) Within the spectral region given by transmittance data, $\log[\alpha(h\nu)]$ displays a "mathematical integral-like shape" $(\int)$, where $\alpha(h\nu)$ is the absorption coefficient of the semiconductor.

The restriction (a) finds its justification on the validity of the single-effective-oscillator approach [13], as stated above. The restriction given in (b) lead us to investigate families of functions where the integral-like shape is present. Let $\mathcal{F}(\gamma, \eta)$ be the set of twice continuously

9

differentiable functions $\psi : \mathbb{R} \rightarrow \mathbb{R}$ such that:

(i) $\psi(0) = \gamma$;

(ii) $\psi'(0) = \eta$;

(iii) $\psi''(0) = 0$;

(iv) $\psi'(t) \geq 0$ for all $t \in \mathbb{R}$.

(v) $\psi''(t) > 0$ if $t < 0$ and $\psi''(t) < 0$ if $t > 0$.

It is easy to see that, given $\psi_-, \psi_+ \in \mathcal{F}(\gamma, \eta)$, the function ψ defined by

$$\psi(t) = \psi_-(t) \text{ if } t \leq 0$$

and

$$\psi(t) = \psi_+(t) \text{ if } t \geq 0,$$

also belongs to $\mathcal{F}(\gamma, \eta)$. This property allows one to define functions that satisfy the properties (i)–(v) and are not odd. We selected four functions $\theta_j \in \mathcal{F}(\gamma_j, \eta_j)$, $j = 1, 2, 3, 4$, choosing γ_j and η_j in such a way that $\theta_j([E_{min}, E_{max}]) \subset [0, 1]$, where E_{min} and E_{max} are the minimum and the maximum photon energy in the spectrum under consideration, corresponding, respectively, to the maximum and minimum wavelength. Finally, we propose the following form for the logarithm of the absorption coefficient:

$$\text{LogModel-}\alpha(h\nu) = \sum_{i=1}^{4} a_i \theta_i[b_i(h\nu - c)] + k. \tag{12}$$

As mentioned above, from the model of the refractive index (3)

$$\frac{1}{n^2 - 1} = \frac{m}{\lambda^2} + \beta,$$

yields

$$\text{Model-}n(\lambda) = \sqrt{\frac{1}{\frac{m}{\lambda^2} + \beta} + 1}. \tag{13}$$

10

We can define new variables, depending on m and β, so that they are computational more insightful. Indeed, once m and β are fixed, we define p and q through $p = n_{m,\beta}(\lambda_{min})$ and $q = n_{m,\beta}(\lambda_{max}) - n_{m,\beta}(\lambda_{min})$ (the inverse relation being quite simple). From this definition it is clear that $p > 1$ and $q > 0$.

The meaning of the parameters a_j, b_j, c, k, p and q are geometrically obvious. Observe that in this way, with $b_j, a_j > 0$, the resulting function has necessarily the integral shape, being c the location of the inflection point. The functions θ_j used in our model were the following:

$$\theta_1 = \begin{cases} \dfrac{2}{4+\pi}\left(\arctan(\overline{h\nu}) + \dfrac{\pi}{2}\right) & \text{when } \overline{h\nu} < 0, \\[4mm] \dfrac{2}{4+\pi}\left(\operatorname{arctanh}(\overline{h\nu}) + 2\right) & \text{when } \overline{h\nu} > 0, \end{cases}$$

$$\theta_2 = \begin{cases} \dfrac{1}{4}\left(\dfrac{4}{1+e^{-\overline{h\nu}}}\right) & \text{when } \overline{h\nu} < 0, \\[4mm] \dfrac{1}{4}\left(\operatorname{arctanh}(\overline{h\nu}) + 2\right) & \text{when } \overline{h\nu} > 0, \end{cases}$$

$$\theta_3 = \begin{cases} \dfrac{1}{3}\left(\tanh(\overline{h\nu}) + 1\right) & \text{when } \overline{h\nu} < 0, \\[4mm] \dfrac{1}{3}\left(\operatorname{arctanh}(\overline{h\nu}) + 2\right) & \text{when } \overline{h\nu} > 0, \end{cases}$$

$$\theta_4 = \begin{cases} \dfrac{1}{3}\left(2\displaystyle\int_{-\infty}^{\overline{E}}\left(1 - \dfrac{1}{1+e^{-t^2}}\right)dt + \sigma\right) & \text{when } \overline{h\nu} < 0, \\[4mm] \dfrac{1}{3}\left(\operatorname{arctanh}(\overline{h\nu}) + 2\right) & \text{when } \overline{h\nu} > 0, \end{cases}$$

where $\overline{h\nu} = 10\left(\dfrac{h\nu - h\nu_{min}}{h\nu_{max} - h\nu_{min}}\right) - 5$ and $\sigma = \displaystyle\int_{-\infty}^{\infty}\left(1 - \dfrac{1}{1+e^{-t^2}}\right)dt.$

The choice of these functions came from intensive experimentation with computer generated films, after discarding many other ones with similar topological properties.

Using (12), (13) and the formulae (4-9), and given a trial thickness d and the parameters a_i, b_i, c, k, m and β a theoretical transmittance $T^{theor}(\lambda)$ can be computed. Given a set of observations $T^{meas}(\lambda_i), i = 1, \ldots, m$, the objective is to solve the following minimization problem:

$$\text{Minimize} \sum_{i=1}^{m} [T^{theor}(\lambda_i) - T^{meas}(\lambda_i)]^2. \tag{14}$$

The objective function (sum of squares) of (14) will be called $F(d, c, k, M, B, a_1, \ldots, a_4, b_1, \ldots, b_4)$. It has 13 variables and we must take into account that all of them must be positive, except, perhaps, c and k. The function has many local minimizers, therefore the optimization procedure is not straightforward, since the application of an ordinary minimization algorithm will normally lead to a local-non-global solution of (14). Below, the optimization procedure used for solving (14) is described.

Assume that we have lower and upper bounds for each variable, except for a_i and b_i, for which we only have an initial estimate and we know that they are nonnegative. The lower and upper bounds for variables d, c, k, p, q are $d_{\min}$, $c_{\min}$, $k_{\min}$, $p_{\min}$, $q_{\min}$ and $d_{\max}$, $c_{\max}$, $k_{\max}$, $p_{\max}$, $q_{\max}$, respectively. The first stage of the optimization procedure defines a *coarse grid* in $[d_{min}, d_{max}]$. For each trial thickness d_{trial} belonging to this coarse grid, we consider the function F which, now, depends on 12 parameters. Then, we define a grid G in the four-dimensional box

$$[c_{min}, c_{max}] \times [k_{min}, k_{max}] \times [p_{min}, p_{max}] \times [q_{min}, q_{max}].$$

For each point of G, we evaluate F and discard the points for which the objective function value is greater than a tolerance $TOL1$. In this way, we obtain a second grid $G' \subset G$. We use each point of G' as initial estimate for minimizing F using the software BOX-QUACAN (see [18,19]) and perform just *one* iteration of this local minimization method. Then we discard a percentage $TOL2$ of the points of G' with worse objective function value. In this

way, we have a third grid $G'' \subset G$. Each point of G'' is then used as initial estimate of BOX-QUACAN for a complete local minimization procedure. The final point for which we have the smaller functional value is, so far, preserved as the representative point for the trial thickness d_{trial}.

So, at the end of the coarse-grid procedure, we have a representative set of parameters and a functional value for each trial thickness. Taking into account the best values of the function, we define a new interval $[d'_{min}, d'_{max}] \subset [d_{min}, d_{max}]$ and a new *fine grid* in this new interval. For each trial thickness in this fine grid (using as initial estimate the point obtained at the end of the Coarse grid step) we directly apply the algorithm BOX-QUACAN set up for a full local minimization. Finally, we fix the thickness with the smallest objective function value and perform the same strategy used in the coarse-grid step (for fixed thicknesses) with the size of the grid G slightly increased. The set of parameters that give the lower functional value is considered to be the estimate provided by our method.

The computer parameters used in the above procedure are:

- for the bounds we used $[c_{min}, c_{max}] = [k_{min}, k_{max}] = [-10, 10]$ while for p, q we used $[p_{min}, p_{max}] = [1.1, 5]$ and $[q_{min}, q_{max}] = [0, 5]$. Although a_i and b_i are not bounded, computational we restricted ourselves to the box $[0, 10]$.

- for the grid G we used 81 equally spaced points in $\mathbb{R}^4$ (meaning that we had $ESP = 3$ equally spaced points at each coordinate). Once we have found and fixed the retrieved thickness (as described above), the size of the improved grid at the last step is $ESP+2$.

- for the fine-grid, we used, respectively, for the lower and upper bound $d_{coarse} - 19$ and $d_{coarse} + 19$ with step 1, where d_{coarse} is the thickness obtained at the end of the coarse-grid step;

- for the tolerance $TOL1$ we used the value 10;

- for the percentage of discard $TOL2$ we used 0.1. Let $s(X)$ be the number of points of the grid X. Then $s(G'') = \max\{0.1\ s(G'), 10\}$. Clearly, this could lead $s(G'')$ into a

13

fraction, had we not the help of the mod function.

C. Experimental and results

The a-Si and a-Si:H films were deposited onto 7059 glass held at 250 ^{0}C with a deposition rate of 1 Å/sec. The rf-sputtering technique was used to produce the H-free a-Si layers, whereas a-Si:H thin films were made by the plasma enhanced chemical vapor deposition method (PECVD). Under these deposition conditions the films are believed to be homogeneous and possessing flat parallel faces. For the growth of a-Si films the deposition conditions were kept identical, only the deposition time being varied in order to produce films with different thickness but otherwise similar. The a-Si:H films originate from two deposition runs made at different times, but believed to be representative of state of the art a-Si:H. The transmittance of the films (400 - 2000 nm range) was measured in a Hewlett Packard Lambda-9 model spectrophotometer, with typical speed 60 nm/min and variable slit. Figures 3 and 4 show the transmittance of thin a-Si and a-Si:H films, respectively. They clearly indicate that envelope-like methods are of no use with these fringe-free transmission spectra. The transmittance of a relatively thick a-Si film has also been included in Fig.3. It displays an absorption modulated interference pattern and can not be treated with envelope-like methods either. The study of films with $d > 100$ nm has been included in the present study for reasons that will become clear in the coming sections. The estimation problem of these relatively thick films has been done using the PUM approach and not the FFM method, used for all the $d < 100$ nm films investigated here. The reasons for the choice of the FFM algorithm in the calculation of films having a thickness $d < 100$ nm were already given and will be discussed in the coming section.

Table I shows the results of the minimization process for all the samples discussed in this contribution. The series include six very thin layers, three of a-Si and three of a-Si:H. The results referring to two thick samples $d > 100$ nm are also included in Table I. In all cases the optimal retrieved thickness is close to that estimated from the deposition rate and

deposition time ($d < 100$ nm) or to values given by a profilometer ($d > 100$ nm). The quadratic error (11) corresponding to the optimum thickness is given in the last column of Table I.

The study of amorphous films with $d > 100$ nm is justified by the need to compare the optical constants of more bulky layers with those retrieved in very thin films. Note that the optical properties of thick films are much less affected by defective interfaces and surfaces than those of very thin layers. The thickness of the defective a-Si:H/substrate interface layer has been estimated to be, at least, of 50 to 100 Å [20]. Deviations to the ideal model adopted in the present study (4) are, then, expected to be smaller in films of thickness $d > 100$ nm. The need to incorporate rather thick films in the present study is also justified by the fact that the bulk properties of both, a-Si and a-Si:H, are known, and the correctness of the retrieval process may be verified. The agreement between the optical properties of a 0.5 μm thick a-Si:H film, retrieved using PUM and those measured on the same films by independent methods, such as photothermal deflection spectroscopy and ellipsometry, has already been published [21,8]. A similar verification procedure becomes almost impossible in the case of very thin amorphous layers.

Figure 5 shows the retrieved values of the absorption coefficient and of the index of refraction of two PECVD a-Si:H films of thickness 624 nm (PUM) and 72 nm (FFM method), respectively, deposited under identical conditions [8]. The retrieval of the properties of sample #7 (see Table I) has been done using both PUM and FFM methods, the final result being identical. The figure clearly indicates that the retrieved optical properties of these two films having quite different thickness are essentially the same, as expected for films deposited under identical nominal conditions but different deposition time. Note that the retrieval does not depend on the use of the PUM or the FFM method for the film having a thickness $d = 72$ nm. It is important to remark: a) The absorption coefficient is perfectly retrieved for both samples, the retrieval interval depending on film thickness, as expected. The retrieval of α at decreasing photon energies fails when a break occurs in the smooth α vs E curve. The break is followed by an almost constant value of α. b) Due to the adoption

15

of (13), the use of FFM for very thin films leads to an unimpeded increase of the index of refraction n as the photon energy approaches the value of the single-effective-oscillator energy. As a consequence, valid n values are only those corresponding to photon energies well below E_{osc}, say $h\nu \lesssim E_{osc}/2$.

Figures 6 and 7 show the retrieved optical constants of a-Si and a-Si:H films, respectively. It is noticed in Fig. 6, that the absorption coefficient differs between samples at photon energies smaller than around 2 eV. For $h\nu > 2$ eV, the retrieved α displays a unique behavior, irrespective of film thickness. In contrast, the retrieved index of refraction depends on film thickness in the whole energy range. Note, again, the unimpeded increase of n with photon energy, a consequence of the functional variation adopted for the index (13). The situation depicted in Fig. 7 refers to two very thin PECVD a-Si:H films deposited under standard PECVD conditions. There is no fundamental difference in the retrieved index of refraction between a-Si:H samples. The absorption coefficient, however, appears to depend on film thickness. In the discussion to follow, likely reasons behind this behavior will be advanced.

D. Discussion

Homogeneous, isotropic, perfectly flat, and parallel-face semiconductor films are a mathematical fiction, in particular when dealing with very thin films. Substrates on which films are formed are neither mathematically plane nor inert, in the sense that their structure may exert a profound influence on the form of the overlying film. The condensed atoms of films prepared by sputtering or chemical vapor deposition possess a surface mobility resulting in an aggregated, rather than a continuous structure. In early measurements of optical constants, for which it was assumed that the film behaved as a thin slice of bulk material, values obtained for the optical constants were found to differ widely from those of the bulk [22]. It is now established that such apparent variations are due to the aggregated structure which is observed in matter of thin layers. Thus, the model idealized in Fig. 1 and (4), is not in practice realized. In other words, the four layer model adopted here to represent the actual

16

experimental situation of very thin film is only approximate, because it does not include some important experimental facts that may affect the retrieval process in a variety of ways. Among other things, the ideal model is only approximate because it does not consider the existence of a substrate/film interface which, in the case of amorphous silicon films, is always a highly perturbed region . The transmittance data contain, in an unknown proportion, the optical properties of the bulk material and of this interfacial region, the thickness of which may depend on preparation conditions and on the nature of the substrate. Such interface is not easy to model, nor its influence to quantify, although it clearly increases as the film thickness decreases. The thinner the film the larger the contribution of the interface layer. Besides this unavoidable effect, the bulk of the films may be inhomogeneous, in the sense that it may contain regions having structurally different materials, or a density deficit, or impurity aggregates, etc. We do not expect this to be the case of the present amorphous silicon films.

In situ ellipsometry has been a powerful experimental tool to investigate the surface layer during the deposition of semiconductor films. By measuring the intensity and polarization of light reflected from the surface, the optical constants of the film are retrieved. The evolution of the real and imaginary parts of the global dielectric function can be followed as the film growth occurs [23]. The data on the nucleation and growth of amorphous silicon films indicate the existence of two regimes [20]. The first, of typically a few hundred angstroms, is when nucleation on the substrate surface takes place. In this regime the measured dielectric constant receives contributions from both the film and the substrate [23] and a model assuming the growth of a uniform layer is unable to explain the experimental data. The second regime corresponds to later stages when the substrate is no longer detectable and only the properties of the top bulk material are probed. In the first regime, the changes of the optical properties with film thickness are dramatic, as they evolve from those of the substrate to those of the bulk material. In the second regime, there is no change of the optical properties of the film, unless its structure changes with increasing thickness. Furthermore, for thin amorphous semiconductor coatings, even when carefully prepared and measured,

17

surface roughness, which originates in the nucleation process, cannot be physically removed from the sample. The surface roughness of the films is also obtained from ellipsometry and a typical roughness of 10 Å is found for optimized a-Si:H films, whereas sputtering deposition leads to a much greater value [20]. These considerations imply that, although the films have been deposited under similar nominal conditions, we should not expect retrieving identical properties as their thickness decreases. This proves to be the case. For the sake of clarity, let us discuss separately the results obtained on a-Si films from those on a-Si:H films.

a. Hydrogen-free amorphous silicon films   The optical properties of sample #4, $d = 491$ nm (see Table I), retrieved with PUM, agree well with published data on a-Si [24]. Note that, besides convexity, the PUM algorithm does not impose any functional dependence of the index of refraction on photon energy. Sample #4 is thick enough to minimize the effects that surface and interface layers may introduce. A test of the goodness of the retrieval process for n is given by its agreement to the single–effective–oscillator model, known to be valid for amorphous semiconductors [13,14]. The model predicts a linear dependence of $1/(n^2 - 1)$ vs $(h\nu)^2$, as shown in Fig. 8 for sample #4. The best linear fit to the retrieved data gives for the single-oscillator-effective energy $E_{osc} = 3.0$ eV, which is near the main peak of the ε_2 spectrum of a-Si. This value compares well with that reported by Wemple for a-Si, $E_{osc} = 3.1$ eV [14]. The dispersion energy extracted from Fig. 8 is $E_d = 37.4$ eV, comparable with Wemple's 34 eV [14] and Chittick's 38.6 eV [25], found by independent methods. Moreover, from the retrieved absorption coefficient it is possible to estimate an exponential-like behavior of the log α vs photon energy. Its slope, $E_U \sim 230$ meV, is in agreement with values normally found in H-free a-Si films. Finally, the E_{04} optical gap, i.e., the photon energy at which α equals 10^4 cm^{-1}, is 1.38 eV, also in agreement with the expected value. Finally, let us note here that the film thickness given by a profilometer, $d = 504 \pm 20$ nm, is close to the retrieved one. We take these results as indicative that the retrieval of the optical constants and the thickness of sample #4 has been successful.

Let us now consider the retrieved values for the very thin a-Si films. The behavior of the refractive index of these films, in the $0.5 < E < 2.0$ eV spectral region is similar in

shape to that of the thickest $d = 491$ nm layer. Figure 6, however, shows that the value of n decreases as the film thickness decreases, a trend indicating a less dense material as the thickness of the films decreases. This result is consistent with the previous discussion referring to nucleation mechanisms of a-Si.

In situ ellipsometry models the dielectric function of very thin films using the Bruggeman effective medium approximation, which considers two components for the dielectric function of the system [20]. Deviations to the model of a uniform growth of the amorphous film are attributed to two microstructural effects: buried layers at the substrate interface of lower density than the bulk material and increase in surface roughness. The adatom mobility of sputtered Si atoms is smaller than that of a-Si:H. As a consequence, both the defective interface region and the surface roughness become larger. The roughness of sputtered a-Si has been found to be particularly important, of the order of 2 nm. The void structure at the interface is also large and may be present in the first 20 nm growth. These experimental findings suggest that the retrieved decreasing n for very thin a-Si layers is the consequence of the growing influence of a density deficit region at the film/substrate interface, as the thickness of the film decreases. The explanation is also consistent with the augmented absorption at photon energies smaller than that of the pseudo-gap. Void-rich regions at the interface increases the density of localized electron states in the pseudo-gap and broaden the tail of states of the valence and of the conduction bands, leading to an augmented optical absorption at energies below the band-to-band transitions [26]. As a complement to the above we show in Table II some physical parameters extracted from the minimization process. Again, the data displayed in Table II illustrate the meaningfulness of the retrieval process.

The present authors are fully aware that the retrieved optical constants and thickness represent average values, in the sense that the model behind the minimization process does not include any kind of film inhomogeneities, which are always present in real physical situations. In spite of the model limitations, the above plausibility arguments lead us to believe that the retrieval of the optical constants of the present very thin a-Si films from

19

transmittance data is meaningful. The results suggest that the FFM method can be applied to transmittance data of amorphous silicon films having a thickness as small as 300 Å.

   b. *Hydrogenated amorphous silicon*   The considerations on the influence of interface and surface inhomogeneities on the overall properties of very thin a-Si films also apply to a-Si:H. Ellipsometry studies show that, due to the different surface mobility of the precursor species, the first nucleation and growth stages in rf-sputtered a-Si and PECVD a-Si:H are not the same [20]. The H-free precursor is more reactive and tend to stick at the landing site. Differently, the precursor species (SiH_3) in a-Si:H PECVD growth has a low sticking coefficient, so that the molecules are continuously adsorbed and released. Hence, the difference between rf-sputtered and PECVD silicon is that the initial inhomogeneities due to nucleation is quickly removed in PECVD growth but remains with rf-sputtered material [27]. The thickness and texture of the density deficit film/substrate interface layer are smaller in a-Si:H than in a-Si, as experimentally found. Hence, thin a-Si:H films are expected to be more homogeneous than H-free layers of similar thickness. Figures 5 and 7 do show that this is indeed the case. The upper half of Figs. 5 and 7 show that there is no significative difference between the retrieved n of the a-Si:H films. Figure 5 also shows that the absorption coefficient of samples #8 (bulky, $d = 491$ nm) and #7 ($d = 99$ nm) are identical within experimental error. The correctness of the retrieved optical properties of sample #8 has been confirmed by independent methods.

   The bottom part of Fig. 7 shows the retrieved absorption coefficient of samples # 5 and #6, two very thin a-Si:H films of another deposition run. The high absorption region ($\alpha \geq 10^5$ cm^{-1}), that mostly probes the film properties after the initial stages of growth, displays identical values for the two films, and are identical of that of the bulk sample #8. An exponential like absorption region is apparent in Figs. 5 and 7. State of the art a-Si:H films possess an exponential absorption edge – or Urbach edge (2) – with a characteristic energy $E_U \sim 50$ meV [27]. The Urbach edge of samples #7 and #8, $E_U \sim 60$ meV, is similar to that given by photothermal deflection spectroscopy (PDS) in thick samples. Figure 7 shows the exponential-like absorption edge for the two thinnest a-Si:H samples.

Sample #6 ($d = 72$ nm) possesses a well defined Urbach edge, with $E_U \sim 45$ meV. This value may originate from a hydrogen content higher than that of samples #7 and #8, which should also provoke a larger E_{04} gap, as found The retrieved Urbach edge of sample #5 ($d = 35$ nm) is very broad, $E_U \sim 85$ meV. It is noteworthy that the FFM method retrieves an exponential absorption edge in a-Si:H films as thin as 350 Å. The broad tail, and the large remaining absorption at photon energies below 1.5 eV of sample #5, is a consequence of the influence of the perturbed film/substrate interface layer, which increases as the film thickness decreases. This layer is a density deficit region containing a void microstructure of unknown characteristics, which contributes, not only to an increased density of deep defects (residual absorption) but also to a larger topological disorder, as evidenced by the broad absorption tail.

It is timely to address now the question of – down to what thickness is it possible to retrieve the properties of very thin films using unconstrained minimization and the adopted model? The numerical [9] and the physical experiments here reported indicate that it is possible to obtain meaningful answers to thicknesses as small as 300 Å. But, even for ideal computer-made films the retrieval process fails for $d < 300$ Å. The failure must not be interpreted as the absence of any response. The problem, detected with computer made films in which the "true" solution is known in advance, is that the thickness coming out of the minimization process is either not the good one, or does not retrieve the expected optical constants. Note that, for *gedanken* films, this failure does not originate from any inadequacy of the adopted model, nor from the presence of defective interfaces (absent in computer experiments), but from the insufficiency of the a priori information on the behavior of the optical parameters. We conclude that the present approach concerning amorphous semiconductor thin films, which considers that α and n possess a functional dependence given by (1)-(3), respectively, is unable to find physically meaningful solution for films having a thickness less than 300 Å. In other words, the certitude that the retrieved thickness corresponds to the correct answer is lost at $d < 300$ Å. At this particular thickness the quadratic error resulting from the minimization process starts flattening, the different

minima corresponding to different thicknesses having close values. We illustrate the point in Fig. 9, which shows, for sample #5, the quadratic error resulting from (11) with a fine 1 nm scan step. It is clear that, although the minimum stays at 35 nm, other neighboring film thicknesses result in not very different quadratic errors, comparable to the one obtained at $d = 35$ nm. The minimization process of samples thicker than 300 nm does not show this behavior (see Fig. 2 for $d = 72$ nm). Similar results are found when dealing with computer made films. The way to circumvent this difficulty, or the kind of a priori information needed to feed the problem in order to solve much thinner films, is not yet known. It represents a next challenge to this sort of ill-posed inverse problems.

E. Conclusions

This work discussed the ways to obtain the optical constants and the thickness of very thin amorphous semiconductor films from spectral transmission data. The use of an approximate, though simple, functional dependence of the index of refraction and of the absorption coefficient on photon energy is given as an a priori information of this reverse optical engineering problem. The optimization process looks for a thickness that, subject to the physical input of the problem, minimizes the difference between the measured and the theoretical spectra. We used a minimization algorithm introduced in [18]. The present method allows retrieving physically meaningful solutions for amorphous semiconductor thin films, as suggested by comparison with known data or with optical parameters measured by independent methods. H-free a-Si and hydrogenated a-Si:H thin films of thickness $d < 100$ nm were studied. It was possible to retrieve physical meaningful estimates for films as thin as 300 Å. The paper discusses the influence of surface and interface regions on the retrieved optical constants and indicates the shortcomings of the adopted model. The limitations of the minimization algorithm used in the present contribution are identified. Their overcoming constitute a new challenge in this important area of very thin optical coating metering.

F. Acknowledgments

REFERENCES

[1] I. Chambouleyron and J. M. Martínez, Optical properties of dielectric and semiconductor thin films, in H. S. Nalwa (ed.), *Handbook of Thin Film Materials*, Vol. 3 (Academic Press, San Diego, 2001), 593-622.

[2] I. Chambouleyron, J. M. Martínez, A. C. Moretti and M. Mulato, *Applied Optics* 36, 8238 (1997).

[3] E. G. Birgin, I. Chambouleyron and J. M. Martínez, *Journal of Computational Physics* 151, 862 (1999).

[4] J. C. Manifacier, J. Gassiot and J. P. Fillard, *J. Phys. E: Sci. Instrum.* 9, 1002 (1976).

[5] A. M. Goodman, *Applied Optics* 17, 2779 (1978).

[6] R. Swanepoel, *J. Phys. E: Sci. Instrum.* 16, 1214 (1983).

[7] R. Swanepoel, *J. Phys. E: Sci. Instrum.* 17, 896 (1984).

[8] M. Mulato, I. Chambouleyron, E. G. Birgin and J. M. Martínez, *Applied Physics Letters* 77, 2133 (2000).

[9] E. G. Birgin, I. Chambouleyron, J. M. Martínez and S. D. Ventura, *Applied Numerical Mathematics* (to appear).

[10] N. F. Mott and E. A. Davis, *Electronic processes in non-crystalline materials*, 2nd Ed. (Clarendon, Oxford, 1979).

[11] J. Tauc, R. Grigorovici and A. Vancu, *phys. status solidi* 15, 627 (1966).

[12] G. D. Cody, The optical absorption edge of a-Si:H, in *Hydrogenated amorphous silicon*, J. Pankove (ed.) Vol. 21B of Semiconductors and Semimetals Series, R; K. Willardson and A. C. Beer, eds. (Academic Press, New York, 1984), pp. 11-82.

[13] S. H. Wemple and M. DiDomenico, Jr., *Phys. Rev.* B 3, 1338 (1971).

[14] S. H. Wemple, *Phys. Rev.* B. 7, 3767 (1973).

[15] E. G. Birgin, PhD Thesis, Institute of Mathematics, State University of Campinas (1998), unpublished

[16] M. Raydan, *SIAM J. Optim.* 7, 26 (1997).

[17] A. N. Tikhonov and V. Ya. Arsenin, *Solutions of ill-posed problems* (Winston-Wiley, New York, 1977).

[18] A. Friedlander, J. M. Martínez, and S. A. Santos, *Appl. Math. and Optim.* 30, 235 (1994).

[19] www.ime.unicamp.br/ martinez

[20] R. W. Collins, Ellipsometric study of a-Si:H nucleation, growth and interfaces, in H. Fritzsche (ed.) *Amorphous silicon and related materials* (World Scientific, Singapore, 1989) pp. 1003-1044.

[21] I. Chambouleyron, E. G. Birgin and J. M. Martínez, in *Optical Interference Coatings 9*, OSA Technical Digest Series, (Optical Society of America, Washington DC, 1998), 132.

[22] O. S. Heavens, *Optical properties of thin films* (Dover Publications, Inc. New York, 1991).

[23] R. W. Collins and J. M. Cavese, MRS Symp. Proc. vol. 118, pp. 19 (Mat. Res. Soc., Pittsburgh, 1989)

[24] D. T. Pierce and W. E. Spicer, *Phys. Rev.* B 5, 3017 (1972).

[25] R. C. Chittick, *J. Non-Cryst. Solids* 4, 1 (1970), as cited in [14]

[26] A. R. Zanatta and I. Chambouleyron, *Phys. Rev.* B 53, 3833 (1996).

[27] R. A. Street, *Hydrogenated amorphous silicon* (Cambridge Univ. Press, 1991).

Table I. Retrieved thickness and quadratic error resulting from the minimization process on H-free and hydrogenated amorphous silicon thin films. The experimental thickness column indicates values either estimated from deposition rate and deposition time, or estimated from profilometer data As indicated, the FFM method has been used for the retrieval of the properties of films with thickness less than 100 nm. Instead, the PUM method has been applied to films with $d >$100 nm.

Sample #	Material	Experimental thick. (nm)	Retrieved thick. (nm)	Quadratic error
1	a-Si	~ 28	30 (FFM)	4.22×10^{-4}
2	a-Si	~ 42	39 (FFM)	3.08×10^{-4}
3	a-Si	~ 58	59 (FFM)	1.15×10^{-4}
4	a-Si	$\sim 504\pm20$	491 (PUM)	1.71×10^{-4}
5	a-Si:H	<50	36 (FFM)	5.14×10^{-4}
6	a-Si:H	~ 80	72 (FFM)	1.19×10^{-4}
7	a-Si:H	~120	99 (FFM)	3.09×10^{-4}
8	a-Si:H	$\sim 620\pm20$	624 (PUM)	1.60×10^{-3}

Table II. Retrieved single-effective-oscillator (E_{osc}) and dispersion (E_d) energies **??** on H-free amorphous silicon very thin films. They are compared with those obtained in the relatively thick sample #4. Remember that the transmittance of samples #1, 2 and 3 has been processed using the FFM method, whereas that of sample #4 has been calculated with PUM. The retrieved E_{osc} and E_d are to be compared with the values found in the literature: $E_{osc} = 3.1$ eV, and $E_d = 38.6$ eV, respectively [14]. The close agreement gives additional support to our belief of the goodness of the retrieval methods.

Sample #	Retrieved thick. (nm)	E_{osc} (eV)	E_d (eV)
1	~ 30	3.4	34.0
2	~ 39	3.5	37.4
3	~ 59	3.3	36.6
4	~ 491	3.0	37.4

FIGURE CAPTIONS

Figure 1: Optical structure considered in this contribution: a very thin 'ideal' amorphous semiconductor film deposited onto a transparent substrate of known index of refraction.

Figure 2: Quadratic error of the difference between measured and retrieved transmittance for an a-Si:H film of thickness 72 nm. Left-hand side: minimization process using a coarse 10 nm scan step. Right-hand side: Same process but using a fine 1 nm scan step in the neighborhood of the minimum found with the coarse 10 nm scan step. The absolute minimum at 72 nm gives the correct thickness of the film.

Figure 3: Transmittance spectra of H-free a-Si films. Note the featureless spectra of films $d < 100$ nm thick. A relatively thick film ($d = 491$ nm) is also shown. Its properties are studied and compared with those estimated from very thin layers.

Figure 4: Transmittance spectra of a-Si:H very thin films ($d < 100$ nm).

Figure 5: Index of refraction (top) and absorption coefficient (bottom) of two a-Si:H films of different thickness retrieved using PUM (thick film) and FFM (very thin film) methods. Note that both films display almost indistinguishable optical constants. The index of the thinner film increases unimpeded as the photon energy increases because of the adopted model for n 3. Note the retrieval of an exponential (Urbach) tail with characteristic energy of $\approx$ 50-60 meV for both films.

Figure 6: Retrieved index of refraction (top) and absorption coefficient (bottom) for a-Si samples. The index n decreases as the films become thinner, a consequence of the increasing influence of a density-deficit layer at the film/substrate interface. The retrieved absorption also suffers the influence of this defective layer, particularly at low photon energy. All films possess an identical absorption at photon energies above 2 eV, at which the most external region of the film is probed.

Figure 7: Retrieved index of refraction (top) and absorption coefficient (bottom) for a-Si: very thin samples. No important differences are found for n between a-Si:H samples. The absorption coefficient, instead, indicates the influence of the perturbed film/substrate interface in the thinner sample, increasing the sub-gap and the residual absorption at low photon energy. This is a consequence of an augmented density of deep localized electron states in the pseudo-gap.

Figure 8: Single-oscillator energy representation vs the squared photon energy for the retrieved n data of the thick ($d \sim 491$ nm) H-free amorphous silicon film. The retrieved parameters are in good agreement with values found in the literature [14,25].

Figure 9: Quadratic error of the difference between measured and retrieved transmittance for an a-Si:H film of thickness 35 nm using a fine 1 nm scan step. Note that, although the 35 nm thickness correspond to a true minimum, neighboring thicknesses give quadratic errors not much different from that at $d = 35$ nm. The a priori information leading to a doubtless response in Fig. 2, seems to be insufficient, or just sufficient, when the thickness approaches 300 Å.
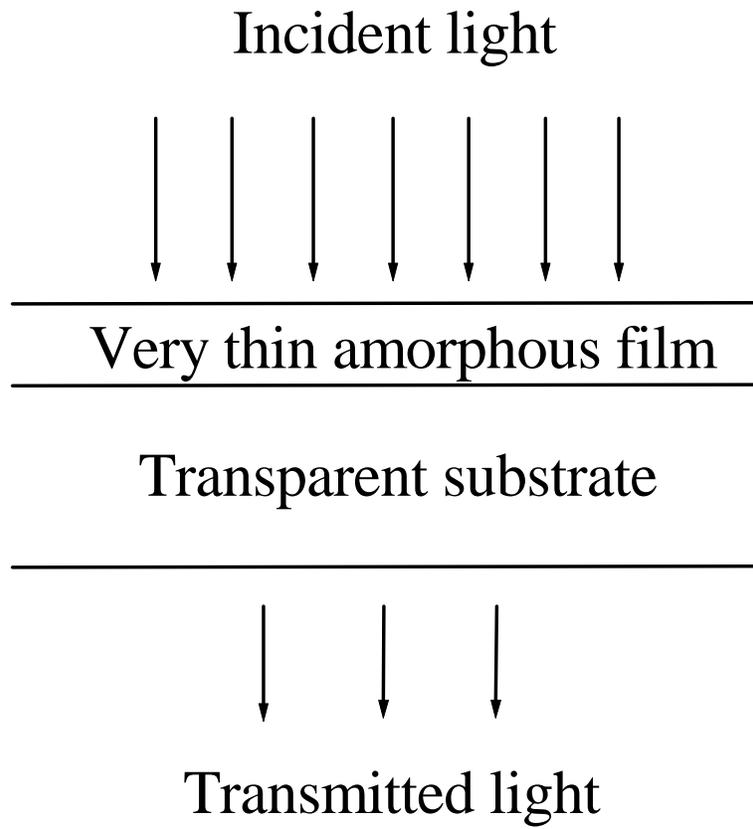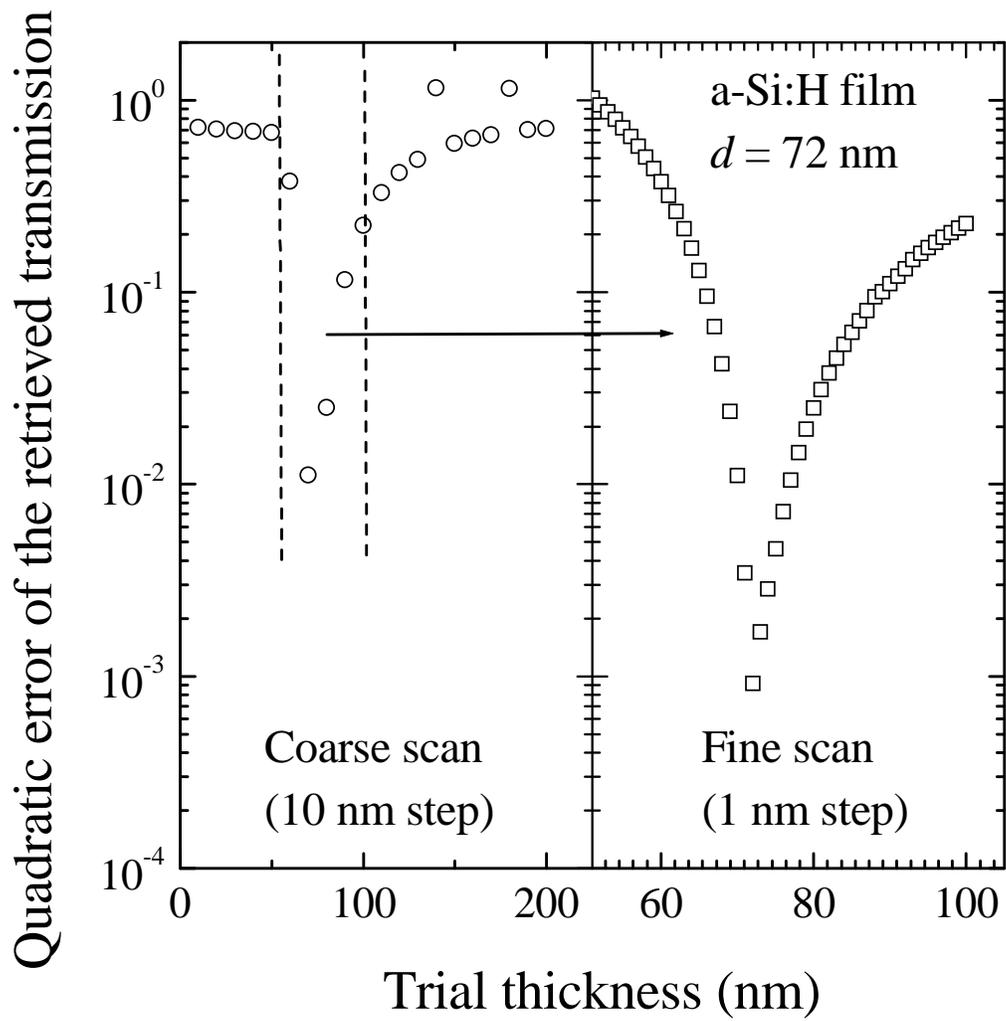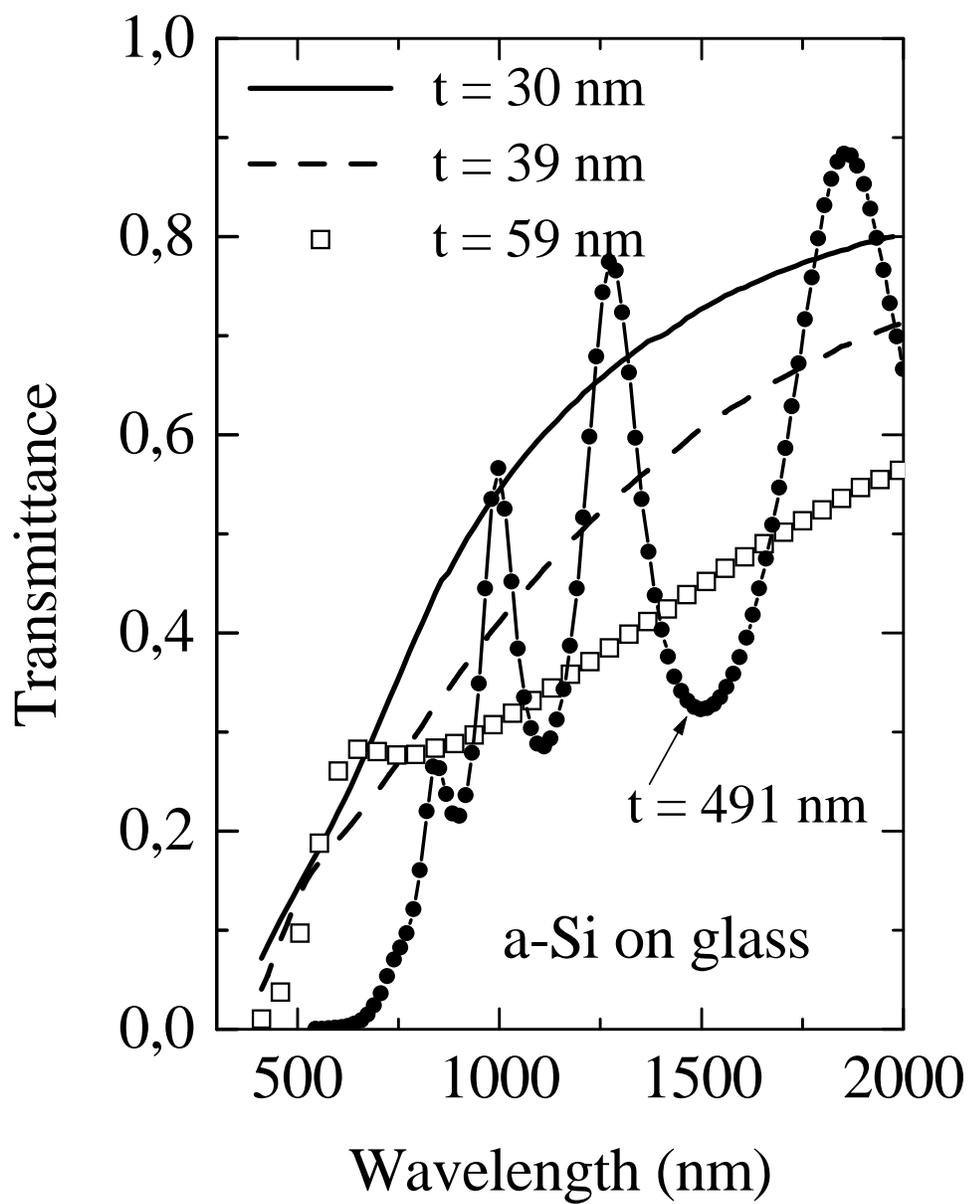
Incident light

Very thin amorphous film

Transparent substrate

Transmitted light

a-Si:H film
$d = 72$ nm

Coarse scan
(10 nm step)

Fine scan
(1 nm step)

Quadratic error of the retrieved transmission

Trial thickness (nm)

Chambouleyron et al.
Figure 3/9

a-Si:H on glass

t = 35 nm
t = 72 nm
t = 99 nm

Transmittance

Wavelength (nm)

Index of refraction

○ t = 99 nm (FFM)
■ t = 624 nm (PUM)

10^6

a-Si:H

Absorption coefficient (cm^{-1})

10^5

10^4

10^3

10^2

1   2   3

Photon energy (eV)

Chambouleyron et al.
Figure 5/9

a-Si on glass

t = 30 nm
t = 39 nm
t = 59 nm
t = 491 nm
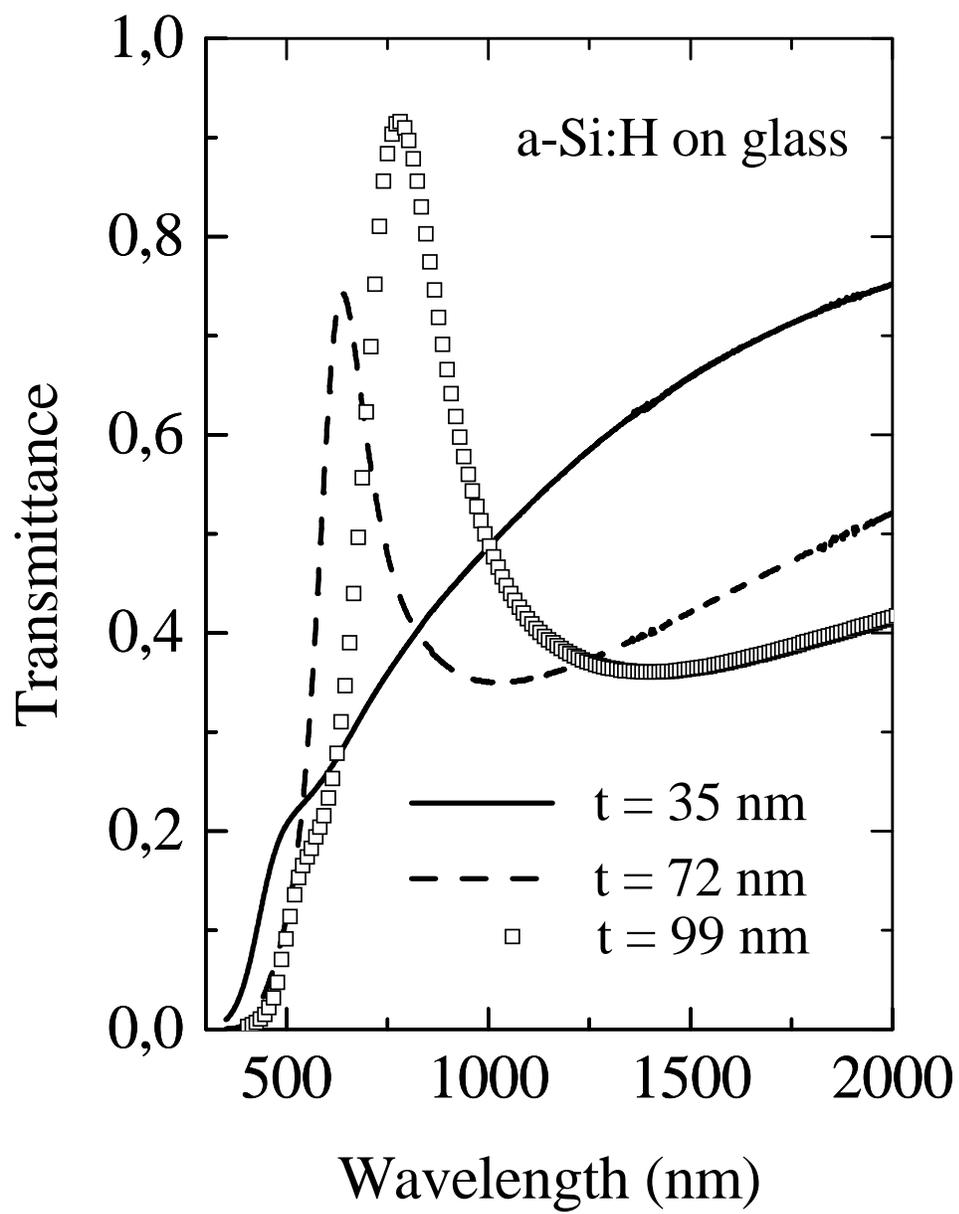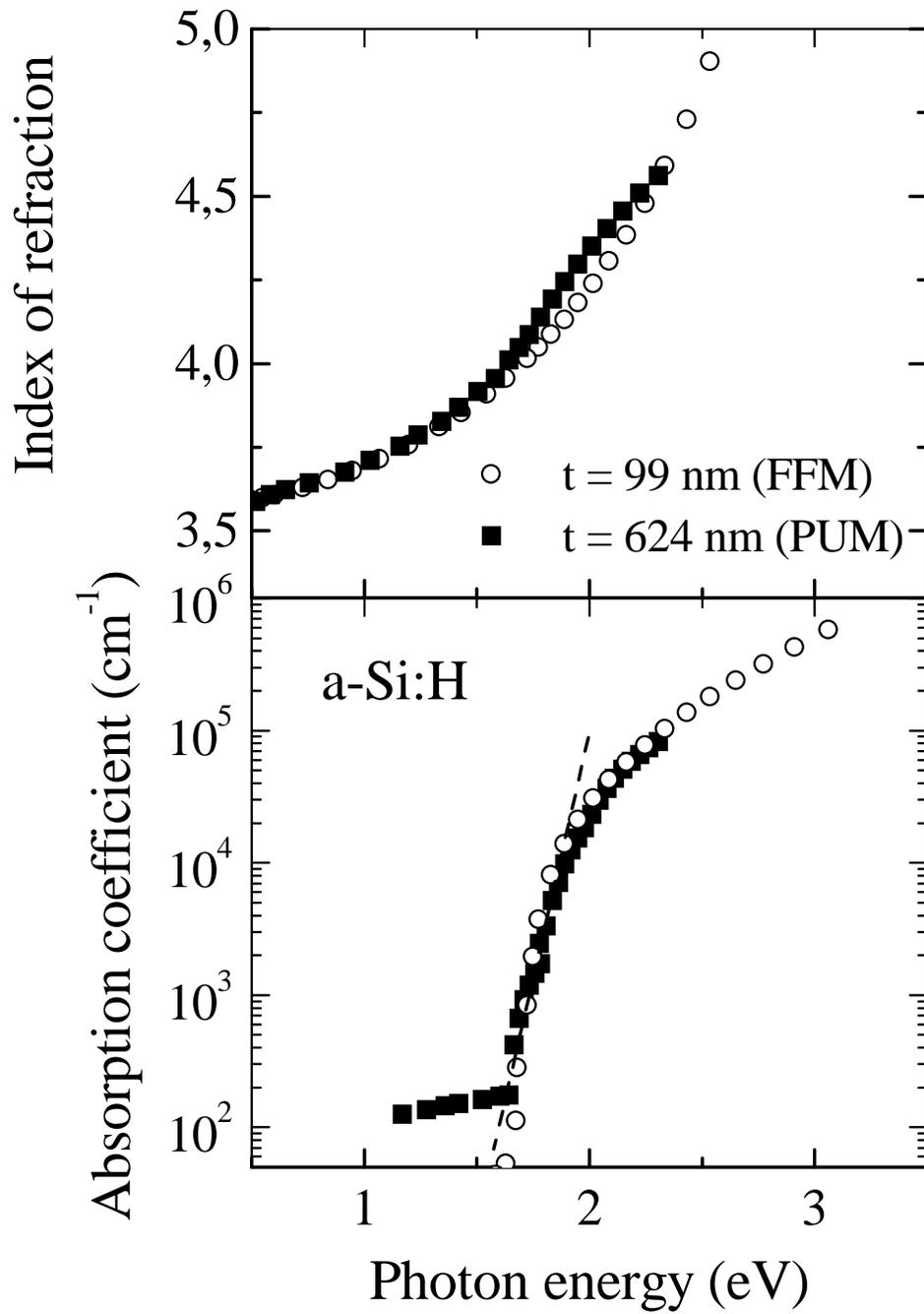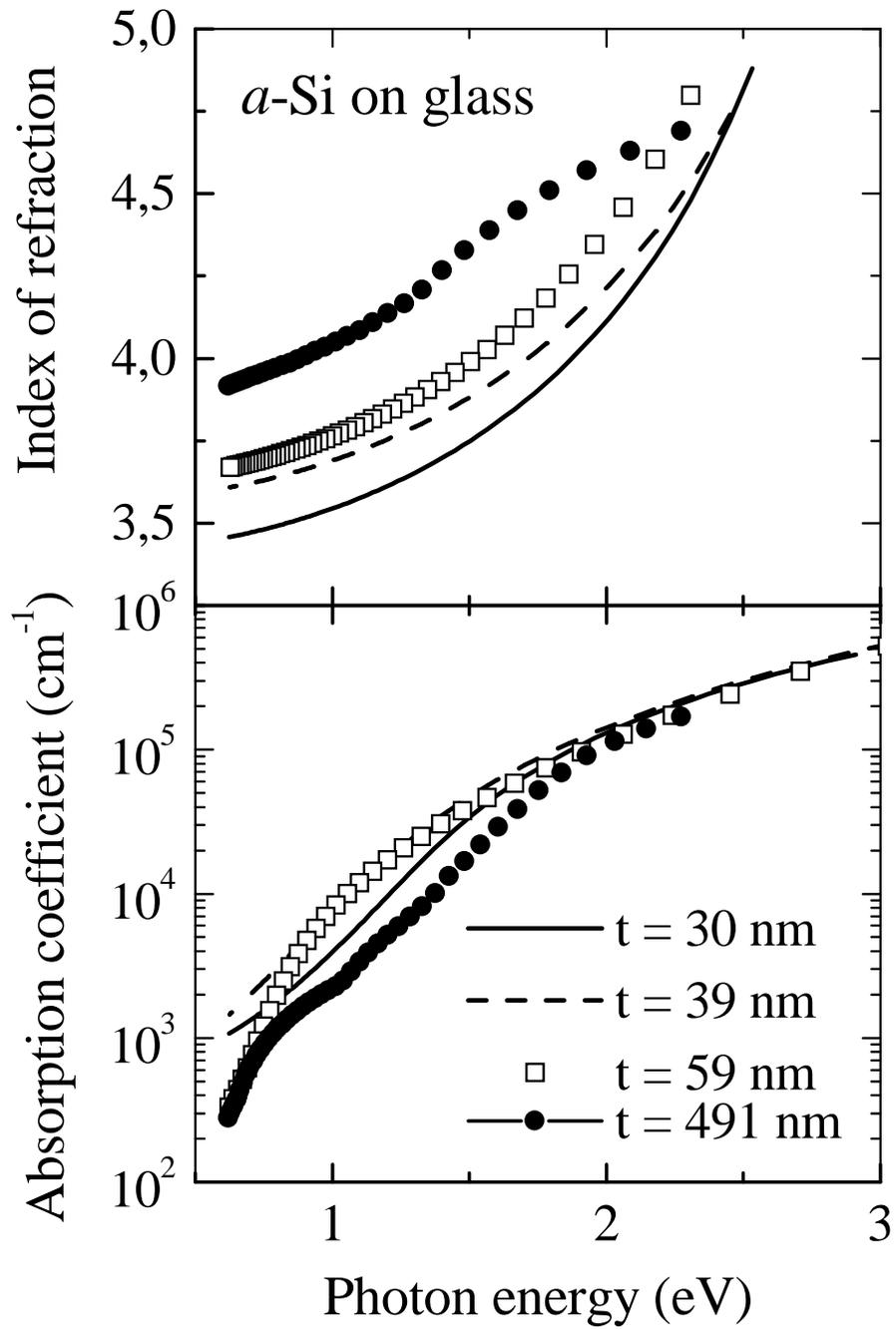
Chambouleyron et al.
Figure 6/9

Chambouleyron et al.
Figure 7/9

a-Si on glass
$d = 491$ nm

$E_{osc} = 3.0$ eV
$E_d = 37.4$ eV

Chambouleyron et al.
Figure 8/9

a-Si:H film

$d = 35$ nm